Experiments in Fluids 1, 83–92 (1983)

Experiments in Fluids

Constant Temperature Hot-wire Anemometer Practice in Supersonic Flows

Part 1: The Normal Wire

A. J. Smits, K. Hayakawa and **K. C. Muck**

Mechanical and Aerospace Engineering Department, Princeton University, Princeton, NJ 08544, USA

Abstract. The performance of a constant-temperature normal hot-wire in a supersonic flow is critically examined. It is shown that this instrument is inherently unsuitable for measuring turbulent temperature correlations because of the highly non-linear response to temperature fluctuations, particularly at low overheat ratios. The instrument is therefore limited to measurements of mean and fluctuating mass-flow rates. Suitable calibration procedures, as well as the limits on spatial and temporal resolution are discussed, and corrections for mean stagnation temperature changes are suggested. The instrument was used to measure the mass-flow fluctuations in a zero pressure gradient Mach 2.9 turbulent boundary layer. A comparison with the available data suggests good agreement.

1 Introduction

Constant-temperature hot-wire anemometers are currently being used in the Gas Dynamics Laboratory at Princeton University to make turbulence measurements in supersonic shear layers. It is considerably easier and faster to use this method than the more widely accepted constant-current anemometer because the constant-temperature mode of operation results in shorter run times which are especially desirable when operating blow-down facilities such as those in use at Princeton. As part of this work, we are engaged in a critical study, both from an analytic and an experimental viewpoint, of hot-wire measurement techniques in compressible flows. In this paper some of our findings on the use of a single normal wire are presented; in a companion paper, Smits and Muck (1983), we discuss the use of an inclined wire.

The present contribution is organized as follows. The hot-wire probe design and the experimental conditions are described in Section 2. In Section 3, an analysis of the hot-wire response is presented, with particular emphasis on the effects of a changing mean stagnation temperature and a varying overheat ratio. The experimental results are given in Section 4 and the conclusions in Section 5.

2 Apparatus and Experimental Arrangements

The current probe design is the result of considerable development. In our first design, bare tungsten wire was spot-welded to the prongs using a tungsten electrode. This proved to be highly unsatisfactory. Not only was the active wire length subjected to aerodynamic interference from the relatively bulky prongs, but it was also difficult to achieve a satisfactory bond between wire and prong, and wire breakages were very frequent. Instead, our current probe design closely follows that recommended by Kovasznay (1950). The tungsten wire (5 μm diameter) is first electroplated with copper and then soft-soldered to the prongs. A dilute sulphuric acid solution is then used to etch away the copper coating and expose an active portion of tungsten wire approximately 0.8 mm long (Fig. 1). To avoid strain-gaging, a small amount of slack is usually introduced. This probe design drastically reduces wire breakage, and in addition, minimizes the interference effect of the bow shocks emanating from the tips of the prongs (Fig. 2).

Fig. 1. Plug-in wire holder. Sketch of current probe design. Wire is tungsten, 2 to 5 μm diameter, 0.8 mm long

The probe was connected to a DISA 55M10 constant temperature anemometer. The overheat ratio was varied by changing the bridge resistance. The frequency response (deduced from a square-wave test) was optimized by ad-

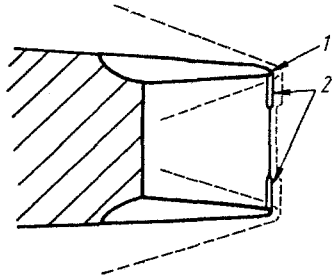

Fig. 2. Detail of probe design, showing approximate shock locations. (Major shocks only). *1* soldered; *2* copper plated stubs

justing the anemometer gain and filter setting. All wires were checked for strain-gaging, and those found to be suspect were discarded.

The anemometer output was separated into a mean and a fluctuating component by low- and high-pass filters each set at 10 Hz. The fluctuating component was digitized directly at 500 kHz sampling rate by a Preston Scientific GMAD-1 A/D converter, and the raw data was stored on-line in the memory of a Hewlett-Packard HP1000 mini-computer for further processing. The mean component of the output voltage was also recorded, along with other mean quantities, by a slower A/D converter.

The wires were tested and calibrated in a small Mach 3 pilot tunnel with a working section measuring 49.3 mm × 44.5 mm. The stagnation pressure was varied between 4×10^5 and 14×10^5 N/m^2 which, for a 5 μm wire, gave a wire Reynolds number range of approximately 80 to 250.

Some measurements were also made in the boundary layer developing on the tunnel floor of the Princeton University 203 mm × 203 mm Supersonic Wind Tunnel. The freestream Mach number was 2.9, the wall conditions were near-adiabatic, and the rms mass-flow turbulence level in the freestream was approximately 1%. The tunnel was operated at a stagnation pressure of 6.9×10^5 N/m^2, which gave a unit Reynolds number of 6.3×10^7/m. At the measuring position, the boundary layer thickness was about 26 mm, with a Reynolds number based on momentum thickness of 77,600.

3 Analysis of the Anemometer Response

In a wide variety of fluid flows the heat transfer from a fine wire filament may be described by the semi-empirical relation

$$\mathrm{Nu}=\frac{H}{\pi l k (T_w-T_e)}=X+Y\,\mathrm{Re}^n \tag{1}$$

where H is the power dissipated in a filament of length l, T_w is the spatially averaged wire temperature, T_e is the wire recovery temperature, and k is the heat conductivity of the fluid. Nu is the Nusselt number, Re is the Reynolds number, and all fluid properties are evaluated at the stagnation temperature T_0. In subsonic flow the parameters X and Y are constant for a given wire at constant Prandtl number, but in supersonic flow they depend on the overheat ratio τ, where $\tau\equiv(T_w-T_e)/T_0$ (Kovasznay, 1950). The exponent n in equation 1 depends on probe design and operating conditions, and generally varies from 0.4 to 0.55. When $n=0.5$, equation 1 is known as King's Law.

As Laufer and McLelland (1956) showed, this wire heat transfer relationship is independent of Mach number for the range $1.2<\mathrm{Ma}<5$ and for Reynolds numbers exceeding 20. The recovery factor $\eta\equiv T_e/T_0$ is then approximately constant, and for our present probe and flow conditions we found $\eta=0.94\pm0.01$.

If we assume that the anemometer bridge (Fig. 3) is perfectly balanced, Eq. (1), in terms of the anemometer output voltage E, becomes

$$\frac{E^2R_w}{\pi k l (R_a+R_w)^2(T_w-T_e)}=Af(\tau)+Bg(\tau)\,\mathrm{Re}^n \tag{2}$$

The parameters A and B are constants for a given wire, independent of the operating point, and the functions f and g are defined by $f=1+f'(\tau)$ and $g=1+g'(\tau)$, where f' and g' are to be found experimentally.

For calibration purposes Eq. (2) may be written in the convenient dimensional form

$$E^2=L+M(\varrho U)^n \tag{3}$$

where ϱU represents the instantaneous mass flow rate along the axis of the probe, and L and M are constants for a particular wire at a given overheat ratio and stagnation temperature.

It must be stressed at this point that in principle, the analysis need not start with a relationship like Eq. (2) or Eq. (3). An arbitrary polynomial curve fitted to the experimental data of E versus ϱU would probably serve equally well, and the sensitivity of the coefficients to a change in wire temperature and stagnation temperature could then be found by further experiment. However, Eq. (2) is to be preferred over such an arbitrary curve fit simply because Eq. (2) has been the subject of considerable research and has received wide experimental support.

To investigate the small perturbation response of the anemometer we may begin by inspecting Eq. (2) and (3). It becomes obvious that it is not generally possible to separate the effect of density and velocity variation; the anemometer responds only to a change in their product, that is, to a change in the mass-flow rate. Thus, for a given wire and a fixed wire temperature, the output is sensitive to $(\varrho u)'$ and T_0', the fluctuations in mass-flow rate and stagnation temperature respectively. Then for small, slow

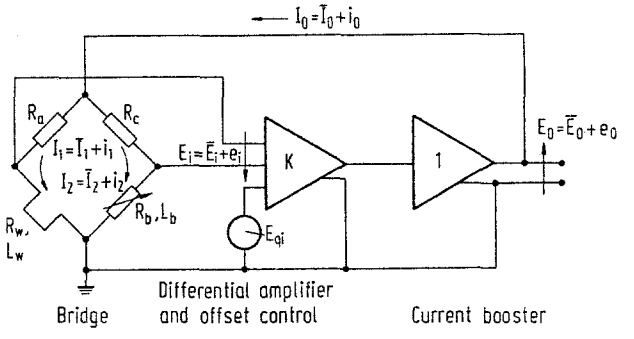

Fig. 3. Constant-temperature hot-wire schematic. Eq_i is the offset voltage, L_b and L_w are the bridge inductance and wire inductance respectively. Typical values: $R_a=R_c/10=50\,\Omega$, $R_w=5\,\Omega$, $L_w=5\,\mu$H

fluctuations the output voltage variation is given by

$$e' = \frac{\partial E}{\partial \varrho U}\bigg|_{T_0} (\varrho u)' + \frac{\partial E}{\partial T_0}\bigg|_{\varrho U} T_0' \tag{4a}$$

i.e.

$$e' = k_m (\varrho u)' + k_\theta T_0' \tag{4b}$$

where k_m is the mass-flow sensitivity and k_θ is the temperature sensitivity [1].

If Eq. (2) accurately describes the heat transfer from the wire, we obtain directly that

$$k_m = \frac{n M}{2E}\left\{\frac{E^2 - L}{M}\right\}^{\frac{n-1}{n}} \quad \text{and} \tag{5}$$

$$k_\theta = \frac{E}{2T_0}\left\{a - \frac{\eta}{\tau} - \frac{(\tau+\eta)}{E^2}\cdot\left[\frac{L}{f(\tau)}\frac{\partial f}{\partial \tau} + \frac{(E^2-L)}{g(\tau)}\frac{\partial g}{\partial \tau}\right] - n b \frac{(E^2 - \mathrm{L})}{E^2}\right\} \tag{6}$$

where we have assumed that the fluid properties vary with temperature according to

$$\frac{k}{k_r} = \left(\frac{T}{T_r}\right)^a \quad \text{and} \quad \frac{\mu}{\mu_r} = \left(\frac{T}{T_r}\right)^b$$

T_r is some reference temperature, and as Kovasznay (1950) suggests, $a = b$ (= 0.768).

The reference temperature T_r is usually taken to be the mean stagnation temperature when this is constant, but if we wish to consider situations where T_0 changes during the experiment, we need to define a constant reference temperature T_c, which we shall call the calibration temperature.

From Eqs. (2), (5) and (6) it is obvious that E, k_m and k_θ are all functions of the wire temperature, stagnation temperature and mass-flow rate. If we fix the wire temperature, a calibration is required to find the output voltage as a function of mass-flow rate and stagnation temperature. Now it is generally straightforward to establish $E = E(\varrho U)$ at a particular T_0, but independently varying the stagnation temperature may present some practical difficulties, especially when we consider the large mass-flow rates that accompany high stagnation pressures. To overcome this problem we suggest the following alternative procedure.

Suppose that $E = E(\varrho U)$ has been found at a given stagnation temperature (= T_c). But, this calibration curve is only valid at temperature T_c. If the stagnation temperature changes by a small amount, the mean mass flow rate can still be found, however, by applying some appropriate corrections. We could either:

(a) use the known calibration constants if the measured output voltage E is corrected according to

$$E_{\mathrm{corr}} = E + \frac{\partial E}{\partial T_0}\bigg|_{\varrho u} (T_c - T_0)$$

i.e.

$$E_{\mathrm{corr}} = E + k_\theta (T_c - T_0) \tag{7}$$

or

(b) use the measured output voltage if the calibration constants L and M are corrected according to

$$L_{\mathrm{corr}} = L_c + \frac{\partial L}{\partial T_0}(T_0 - T_c) \tag{8a}$$

and

$$M_{\mathrm{corr}} = M_c + \frac{\partial M}{\partial T_0}(T_0 - T_c) \tag{8b}$$

where $\partial L/\partial T_0$ and $\partial M/\partial T_0$ can be found from Eqs. (2) and (3).

In addition, the correct mass-flow sensitivity can be found using a similar procedure. We could either:

(a) find the sensitivity from Eq. (5) using the measured output voltage and then correct this sensitivity according to

$$k_{m\,\mathrm{corr}} = k_m + \frac{\partial k_m}{\partial T_0}\bigg|_E (T_c - T_0) \tag{9}$$

where $\partial k_m/\partial T_0$ may be found by differentiating Eq. (5); or

(b) correct the calibration constants as suggested in Eq. (8), and then find the sensitivity from Eq. (5) using these corrected constants and the correct mass-flow rate [i.e. the mass flow rate found after applying the corrections suggested by Eqs. (7), (8)].

All of these correction procedures assume that the functional dependence of the output voltage on the stagnation temperature is known. If we wish to avoid finding this dependence experimentally then we must assume that Eq. (2) accurately models the heat transfer characteristics of the wire. This assumption is probably acceptable for determining the corrections suggested above (as long as these corrections are small), but it becomes less acceptable when the actual temperature sensitivity is required. Before the temperature sensitivity can be calculated with confidence, the accuracy of Eq. (2) and therefore Eq. (6) would have to be established.

The magnitude of the correction required for a change in mean stagnation temperature will depend on the properties of the wire and the operating conditions. Consider a typical wire in a Mach 3 flow with a stagnation pressure of $7 \times 10^5 \mathrm{N/m^2}$ and a stagnation temperature of 270 °K.

1 We have purposely presented equation 4 in dimensional form. Non-dimensional representations (usually expressed in terms of logarithmic derivatives) can lead to confusion when changes in mean stagnation temperature are considered

Table 1. Fractional changes per degree increase in T_0

Overheat ratio	$\frac{\Delta(\varrho U)}{\varrho U}\Big/°\mathrm{K}$	$\frac{\Delta k_m}{k_m}\Big/°\mathrm{K}$
$\tau = 1.0$	0.0026	−0.0028
$\tau = 0.5$	0.0096	−0.0096
$\tau = 0.2$	0.029	−0.029

Some representative values of the fractional change in ϱU and k_m per degree in T_0 are given in Table 1. These values show that the temperature dependence of the calibration increases significantly with decreasing overheat ratio, and also that the temperature dependence cannot be neglected at any overheat because the mean stagnation temperature can vary significantly even within the flow field. For example, Settles et al. (1979) measured a 4% change in stagnation temperature while traversing a Mach 3 zero pressure gradient turbulent boundary layer on an adiabatic wall.

We have already seen that the output voltage fluctuation contains contributions from both mass-flow rate fluctuations and temperature fluctuations. These different contributions can be distinguished because the ratio of the mass-flow sensitivity to the temperature sensitivity is a strong function of wire temperature.[2] This is clearly shown in Fig. 4, where this ratio is plotted for a typical wire at a fixed Reynolds number and stagnation temperature.

From Eq. (4) the mean square variation in output voltage is given by

$$\overline{e'^2} = k_m^2 \left\{ \overline{(\varrho u)'^2} + 2\frac{k_\theta}{k_m}\overline{(\varrho u)' T_0'} + \frac{k_\theta^2}{k_m^2}\overline{T_0'^2} \right\} \tag{10}$$

where an overbar denotes a time average. Equation 10 shows that a minimum of three different wire temperatures are required to determine the three unknowns $\overline{(\varrho u)'^2}$, $\overline{(\varrho u)' T_0}$ and $\overline{T_0'^2}$. More accuracy can be obtained by taking a larger number of readings and using the familiar modal analysis (see for instance, Morkovin, 1956). It may be noted that the data taken at low overheat ratios are particularly important if $\overline{(\varrho u)' T_0}$ and $\overline{T_0'^2}$ are required accurately.

When the overheat ratio of a constant-temperature anemometer is reduced, however, the maximum frequency response decreases, and the response to temperature fluctuations becomes increasingly non-linear.

It is intuitively obvious that the response to temperature fluctuations becomes non-linear at low overheat ratios. The temperature sensitivity is a strong function of τ, Eq. (6), and since the wire temperature is kept constant, fluctuations in stagnation temperature cause τ to vary. When τ is small, a small fluctuation in T_0 produces a fractionally large change in τ and therefore the instantaneous sensitivity can differ significantly from either its static value, or its value at the "average" temperature.

The error in the rms temperature-fluctuation level due to this nonlinearity may be estimated by the following approximate analysis, which extends the work of Smits and Perry (1980). If we assume that the stagnation temperature fluctuations θ are normally distributed with a standard deviation σ ($= \sqrt{T_0'^2}$), then

$$\sigma^2 = \frac{1}{\sigma\sqrt{2\pi}} \int_{-\infty}^{\infty} \theta^2 \exp(-\theta^2/2\sigma^2)\, \mathrm{d}\theta.$$

Consider e_θ, which is the contribution to the instantaneous output voltage due to temperature fluctuations, Eq. (4b). The mean square output voltage due to temperature fluctuations alone is then given by

$$\overline{e_\theta^2} = \frac{1}{\sigma\sqrt{2\pi}} \int_{-\infty}^{\infty} (k_\theta \theta - \overline{e_\theta})^2 \exp(-\theta^2/2\sigma^2)\, \mathrm{d}\theta \tag{11}$$

where k_θ is the temperature sensitivity at temperature $(T_0 + \theta)$, and

$$\overline{e_\theta} = \frac{1}{\sigma\sqrt{2\pi}} \int_{-\infty}^{\infty} (k_\theta \cdot \theta) \exp(-\theta^2/2\sigma^2)\, \mathrm{d}\theta \neq 0$$

since we have taken $\bar{\theta} = 0$ and $e_\theta = k_\theta \theta$. If we write

$$\gamma^2 = \frac{1}{(k_\theta)_{\bar{\theta}=0}^2 \sigma^3 \sqrt{2\pi}} \int_{-\infty}^{\infty} (k_\theta \theta - \overline{e_\theta})^2 \exp(-\theta^2/2\sigma^2)\, \mathrm{d}\theta \tag{12}$$

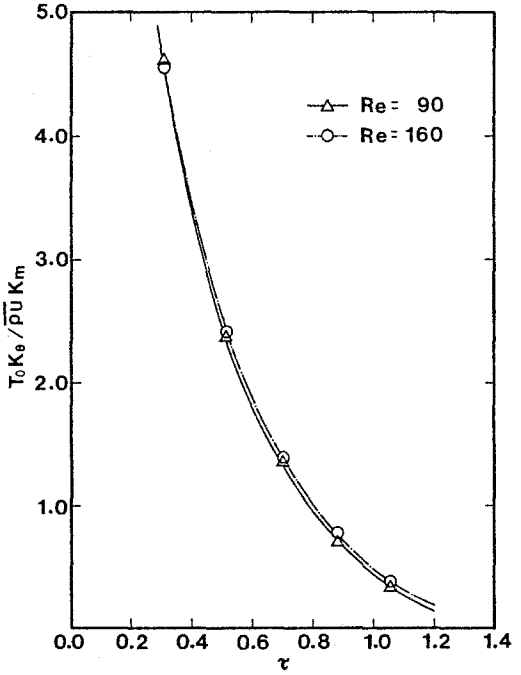

Fig. 4. Relative sensitivity as a function of overheat ratio, shown for a typical wire at two Reynolds numbers

2 Changing the wire temperature changes the overheat ratio if the stagnation temperature is kept constant. It is important, however, to make the distinction between wire temperature and overheat ratio because the former is independent of the stagnation temperature while the latter is not

then γ represents a crude estimate for the error that appears in the rms temperature fluctuation level if the temperature dependence of k_θ is ignored; when γ exceeds one the temperature fluctuation level is over-estimated.

The ratio γ was calculated for a typical tungsten wire ($l = 1$ mm, $d = 5\,\mu$m), and an rms temperature turbulence level of 4% ($= \sigma/T_0$), which is typical of a zero pressure gradient turbulent boundary layer. The sensitivity k_θ was found using an analysis similar to that given by Smits and Perry (1980), with the simplifying assumptions that $\eta = 1$ and $f = g = 1$. The results are given in Fig. 5.

It may be seen from Fig. 5 that the effects of a temperature-dependent gain quickly become significant as the overheat ratio is reduced, particularly when the offset voltage is low. Therefore, a limit on the lowest practical overheat ratio exists; this is the point where the inaccuracies in the temperature measurement become unacceptable.

The non-linear behaviour at low overheat ratios is virtually independent of the feedback gain K (for $K \geqq 200$, say). Therefore, the results of Fig. 5 apply to systems with either a constant gain, or a frequency dependent gain. In systems with a "flat-gain" behavior, the offset voltage plays an important role in adjusting the frequency response. When the amplifier has a frequency-dependent gain, however, the frequency response is controlled by varying the upper frequency roll-off of the amplifier, rather than by adjusting the offset voltage (Smits and Perry, 1980). Nevertheless, Fig. 5 shows that the non-linearity at low overheat ratios can be important, regardless of the value of the offset voltage. In addition, it may be noted that systems which use a frequency-dependent gain display a step in the frequency response at relatively low frequencies. Smits and Perry (1980) showed that the size of this step increases when the overheat ratio and the high-frequency gain of the amplifier are reduced, although it may be significant under all operating conditions. Smits and Perry recommended that such systems be operated with a constant gain.

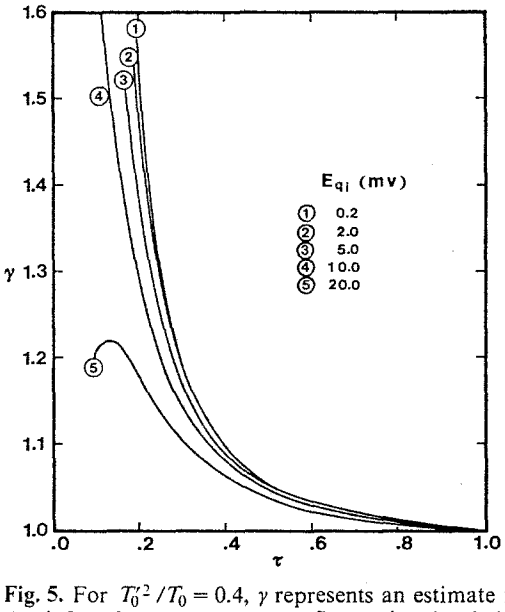

Fig. 5. For $T_0'^2/T_0 = 0.4$, γ represents an estimate for the error in the inferred rms temperature fluctuation level due to the non-linearity of the temperature sensitivity, for different offset voltages

We have thus far ignored the effect of a temperature dependent gain on the measurement of the mass-flow/temperature correlation. It is difficult to be precise, but the error in this correlation is likely to be larger than that given by the ratio γ, because the nonlinear gain will tend to skew the inferred temperature distribution. Thus the lower limit on the overheat required for accurate correlation measurements may well be higher than that required for accurate measurements of the rms temperature-fluctuation level.

Placing a limit on the minimum overheat ratio will adversely affect the accuracy of the modal analysis, however, and it appears that a constant-temperature anemometer is inherently unsuitable for accurate measurements of correlations which involve temperature fluctuations. Therefore, the instrument is only suitable for measuring mass-flow fluctuations, and if temperature fluctuations are present, accurate measurements of $\overline{(\varrho u)'^2}$ are only possible at high overheat ratios. As we see from Eq. (10),

$$\overline{(\varrho u)'^2} = \frac{\overline{e^2}}{k_m^2 (1 + 2\Delta_1 + \Delta_2)} \tag{13}$$

where $\Delta_1 = R\sqrt{\Delta_2}$,

$$\Delta_2 = \left(\frac{k_\theta T_0}{k_m \overline{\varrho U}}\right)^2 \left[\overline{T_0'^2}/T_0^2 \Big/ \overline{(\varrho u)'^2}/\overline{(\varrho U)^2}\right]$$

and $R = \overline{(\varrho u)' T_0'} \Big/ \left(\sqrt{\overline{(\varrho u)'^2}}\ \sqrt{\overline{T_0'^2}}\right)$.

Thus, if the correlations involving T_0' are unknown, Δ_1 and Δ_2 must be made small if we are to avoid errors in the inferred mass-flow turbulence intensity. This requires operation at high overheat ratios, where $k_\theta T_0 \ll k_m \overline{\varrho U}$ (Fig. 4). Of course, the magnitudes of Δ_1 and Δ_2 also depend on the magnitudes of the unknown correlations, but in most flow situations it should be possible to estimate the error in $\overline{(\varrho u)'^2}$ fairly satisfactorily and then set the overheat ratio accordingly.

The upper limit on the overheat ratio depends on the wire material. A tungsten wire will begin to oxidize at a certain temperature, and to avoid this the spatially averaged wire temperature T_w should not exceed 600 °K. When $T_0 = 270$ °K this corresponds to a maximum overheat ratio of approximately 1.10.

We have seen that the temperature sensitivity of the constant-temperature anemometer is highly non-linear at low overheat ratios. If temperature fluctuations are negligible, however, the variation of the frequency response with overheat ratio is still of interest.

We have already noted that, when the overheat ratio is reduced, the maximum frequency response of the constant temperature anemometer is correspondingly decreased. In contrast, the constant current anemometer makes use of a compensating amplifier which can be adjusted to maintain a flat frequency response up to the system roll-off frequency, regardless of the wire overheat ratio[3]. In the constant temperature system, however, this compensation is achieved automatically through a feedback loop, and the maximum frequency response is therefore limited by the system operating conditions.

For a constant temperature anemometer, the anticipated variation of the roll-off frequency with overheat ratio may be deduced using the analysis of Perry and Morrison (1971). The feedback circuit model is shown in Fig. 3. The system frequency response is described by a third-order transfer function if the wire inductance and the bridge balance inductance are non-zero, and the effect of amplifier frequency response is neglected. When the poles of this transfer function all have negative real parts the system is stable, and the roll-off frequency f_R will be proportional to the scalar distance of the dominant pole from the origin. The dominant pole can be real, or it can be one of a pair of complex conjugate poles. At a given operating point the roll-off frequency is generally higher if the system has been adjusted so that the complex conjugate poles are dominant. In fact, Freymuth (1981) suggested that the optimum response (maximally flat) probably occurs when all three poles influence f_R.

Under the conditions of constant Reynolds number, a high amplifier gain and a perfectly balanced bridge, the analysis of Perry and Morrison (1971) can be used to show that f_R is proportional to $\sqrt{\tau}$ when the response is quadratic, and proportional to τ when the response is dominated by a real pole.

This analysis will only be valid, however, if the bridge is perfectly balanced and the amplifier gain and frequency response are sufficiently high. These assumptions implicitly neglect the improvements in the frequency response that are possible when the amplifier gain, the bridge balance inductance and either the high-frequency filter or the offset voltage are adjusted appropriately at each operating point. Freymuth (1981) took these considerations into account, and his analysis suggests that in the optimum case f_R is proportional to $\tau^{1/3}$. Thus, in practice the dependence of f_R on overheat ratio may be rather weak.

To complete the discussion of system frequency response, two additional topics must be considered: end-conduction effects and spatial resolution.

3 This statement is true in principle only. In practice, the compensation amplifier is adjusted by introducing a known perturbation, such as a square wave, in the wire current. If stray bridge inductance is present, Smits (1974) has shown that the compensation level found from current injection can be seriously in error, particularly at low overheat ratios

The influence of end conduction on the frequency response of constant-temperature hot wires operating in subsonic flow has been treated extensively by Perry et al. (1979) and Smits and Perry (1980). In a supersonic flow, however, a detached shock wave forms in front of the wire, bow shocks emanate from the prong tips, and the flow field is rather more complicated. Nevertheless, we believe our current probe design minimizes the effect of the bow shocks by confining their influence to the stubs which support the wire filament. In addition, we are dealing with a flow regime where the hot-wire response is independent of Mach number. These results suggest that the analysis of end-conduction effects in subsonic flow can be used as a qualitative guide for the supersonic case, and the behavior for the most interesting case of high overheat ratio may be briefly summarized as follows.

At high overheat ratios end-conduction effects appear to be associated with asymmetries in the wire temperature distribution. These asymmetries are caused by wire property variations, surface contamination, and bowing of the wire filament, which may be particularly pronounced when the wire is deliberately slackened to avoid strain gaging. As a result, heat waves travel along the wire and reduce its effective time constant. A step in the frequency response occurs, and from tests carried out by Perry et al. (1979) it seems that the associated error in the rms turbulence level can be as high as 10%. No simple solution for minimizing end-conduction effects exists because the effects of end conduction can occur with all wire geometries. Perhaps the only practical answer is to repeat the required measurement a number of times using different wires.

Finally, consider the spatial resolution of hot-wire probes. The small motions in a turbulent flow will have a length scale given by the Kolmogorov length scale η, and in a supersonic shear-layer these motions are typically much smaller than the length of the hot-wire filament l. The hot wire therefore attenuates the small-scale contributions to the turbulence signal and distorts the high frequency end of the spectrum. Wyngaard (1968) made an estimate of this distortion using some simple assumptions about the universal nature of the small-scale motions. His results suggest that, under the worst condition, where $\eta/l \to 0$, the measured one-dimensional spectrum falls to one-half of its true value at a wave number of $2.1/l$. The corresponding frequency, at a Mach number of 3 and a stagnation temperature of 270 °K, is 250 kHz for a wire of length 0.8 mm. This frequency limit could be extended by decreasing the wire length (although there is an obvious limit on the smallest wire length if reasonable l/d ratios are required at the same time). Alternatively the correction procedure suggested by Wyngaard (1968) may be used. Yet, the limited spatial resolution of the hot-wire is not always the most severe restriction on the anemometer response. For our present flow conditions and sampling rates, the frequency limit calculated above coincides with the maximum frequency resolution of the A/D converter,

and both these limits are usually higher than the maximum frequency response of the anemometer. Thus it is the limited frequency response of the anemometer which governs the upper frequency of our turbulence measurements.

4 Results and Discussion

The wires were calibrated in the Mach 3 pilot tunnel described in Section 2. The mass-flow rate was varied by changing the stagnation pressure and the wire temperature T_w was set by selecting the operating wire resistance R_w. T_w was calculated according to

$$R_w = R_{273}\{1 + \alpha(T_w - 273) + \beta(T_w - 273)^2\}$$

where R_{273} is the wire resistance at 273 °K, and α and β are the first and second temperature coefficients of resistivity. The coefficient α was experimentally found to be $0.0038\,°K^{-1} \pm 3\%$. An average value of $1.0 \times 10^{-6}\,°K^{-2}$ was used for β, based on published values (Morkovin, 1956).

During calibration the stagnation temperature usually varied by two or three degrees. The output voltage was corrected for this small temperature variation by the following iterative procedure. A first correction was made by fitting Eq. (3) to the uncorrected data, and using Eq. (6) to calculate k_θ. Equation (7) was used to correct the measured output voltage to a common calibration temperature (usually the average temperature). Then revised estimates for the calibration constants were found by fitting Eq. (3) to the corrected data, which gave a better estimate for k_θ, and so on. In practice, the first iteration was always sufficiently accurate for the small temperature changes encountered during calibration.

Some typical results are given in Fig. 6. For our current probe design we found that Eq. (3) with $n = 0.55$ was an excellent fit to the static calibration data.

By calibrating at different wire temperatures, and correcting each calibration for stagnation temperature drift, the functions $f(\tau)$ and $g(\tau)$ may be found. Figure 7 shows that the linear relationships

$$f(\tau) = 1 - 0.65\,\tau$$

and

$$g(\tau) = 1 - 0.085\,\tau$$

fit the data very well. These results may be compared with those of Kovasznay (1950), who found for his probes

$$f(\tau) = g(\tau) = 1 - 0.18\,\tau.$$

To verify the accuracy of the corrections suggested for mean stagnation temperature drift, a particular wire was calibrated at two different temperatures (270 °K and 280 °K). At a fixed output voltage the corresponding mass-flow rate was found from each calibration, and the ratio is plotted as a function of output voltage in Fig. 8; the ratio of the appropriate mass-flow sensitivities is also shown. The error bars in Fig. 8 indicate the uncertainty in the calibration determined by repeating the calibration a number of times at a given temperature.

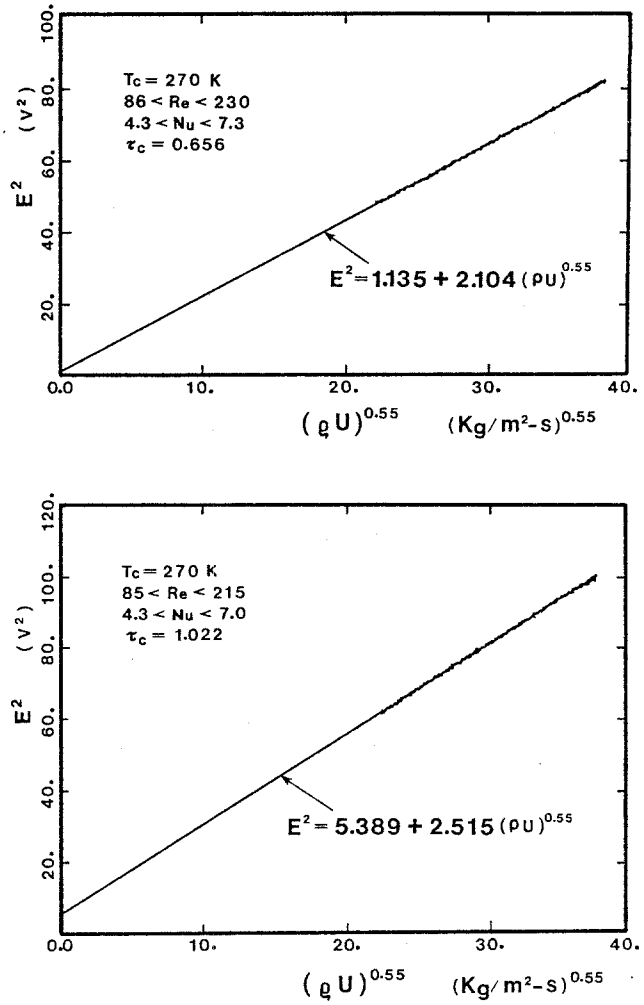

Fig. 6. Two typical normal wire calibrations

The results clearly indicate that variations in the mean stagnation temperature can significantly affect the inferred values of the mass-flow rate and the mass-flow fluctuation intensity.

The experimental results may be compared with those calculated according to the methods described in Section 3 (Fig. 8); the agreement is within experimental error. Thus the corrections proposed for a change in stagnation temperature, Eqs. (7), (8), (9), appear to be sufficiently accurate to account for temperature variations of the order of ten degrees.

To determine how f_R varied with τ, the frequency response was initially optimized at the highest overheat ratio used in the experiment. The overheat ratio was then reduced, first without adjusting the system frequency response, and then by optimizing the frequency response at each overheat ratio.

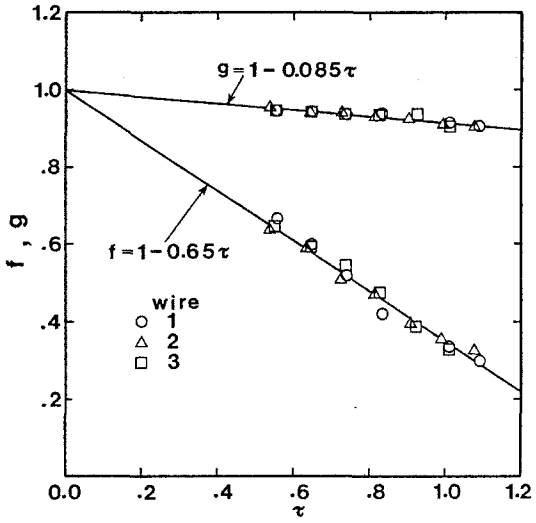

Fig. 7. Proposed correlations for functions $f(\tau)$ and $g(\tau)$

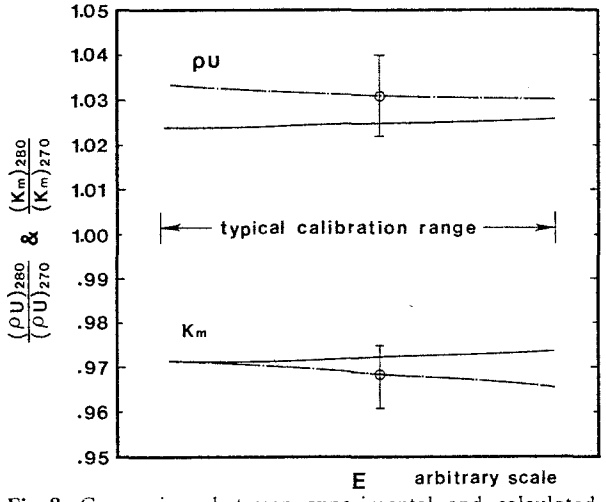

Fig. 8. Comparison between experimental and calculated temperature dependence of hot-wire calibration. The subscript refers to the stagnation temperature at which ϱU and k_m were determined (at a given voltage): —— calculated; –·–· measured

The upper roll-off frequency of the anemometer was found by super-imposing a small amplitude square wave perturbation on the wire voltage. Perry and Morrison (1971) and Freymuth (1977) have demonstrated the usefulness of this method for subsonic flow, and Bonnet (1982) has recently tested the accuracy of the method in compressible flow. He compared the response to a square wave voltage perturbation, a sinusoidal voltage perturbation, and a perturbation in radiant heat flux induced by a frequency modulated laser beam. Bonnet found good agreement between all three methods (for $\tau > 0.1$), and this gave strong support for the accuracy of the square wave test used in the current experiment. Our findings are summarized in Fig. 9.

In Section 3 we predicted that f_R was proportional to $\sqrt{\tau}$ when the system had a quadratic response, proportional to τ when the system was dominated by a real pole, and proportional to $\tau^{1/3}$ when the system was adjusted for optimum response at each overheat. These relationships were scaled appropriately to pass through the first experimental point (where f_R had a maximum value) and were plotted in Fig. 9. We can see that the experimental results lie within the expected range; moreover, the optimum response data agrees well with prediction.

Adjusting the response at each overheat ratio clearly improves the frequency response considerably, and it appears that f_R remains reasonable even at very low overheat ratios. Of course, what constitutes a reasonable value of f_R depends on the experiment. Kistler (1959) found that in a high Reynolds number Mach 2.3 boundary layer, a cut-off frequency $f_R \geqq 5\ (U_\infty/\delta)$ Hz was required for accurate turbulence intensity measurements. Under our experimental conditions (Mach 3, $U_\infty \approx 600$ m/s), according to Kistler's criterion, the corresponding limit on the boundary layer thickness is $\delta \geqq (3 \times 10^6/f_R)$ mm. For the anemometer response shown in Fig. 9, this criterion requires that at $\tau = 0.2\ \delta \geqq 30$ mm, and at $\tau = 1.0\ \delta \geqq 14$ mm.

To demonstrate the constant-temperature hot-wire technique in practice, the mass-flow fluctuation levels in a Mach 2.9 turbulent boundary layer were measured. By comparing the results with data for similar flows, some indication of the measurement accuracy was obtained.

In these measurements, a number of different wires were used, but all wires had a nominal diameter of 5 μm, a length-to-diameter ratio of approximately 150, and the frequency response in the freestream was about 200 kHz in all cases. The boundary layer flow was typical of a zero pressure gradient turbulent boundary layer. Further details of the flow field, and the data acquisition system are given in Section 2.

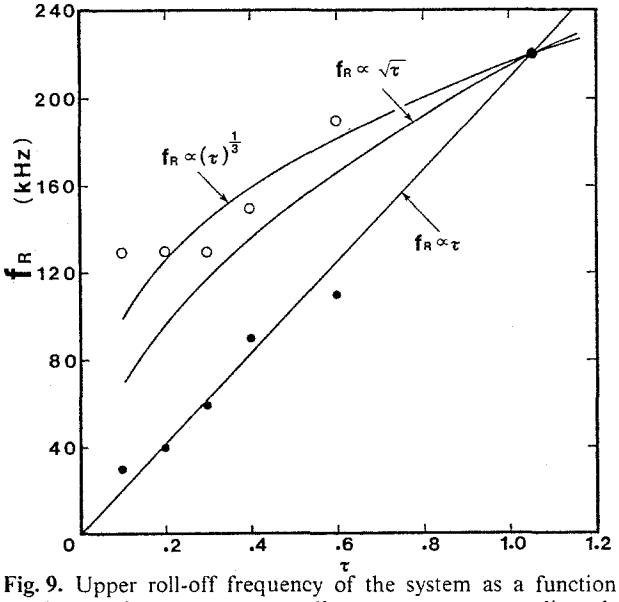

Fig. 9. Upper roll-off frequency of the system as a function of overheat ratio: •, no system adjustment; ○, system adjusted for optimum response at each overheat ($d = 5$ μm, $l/d = 150$)

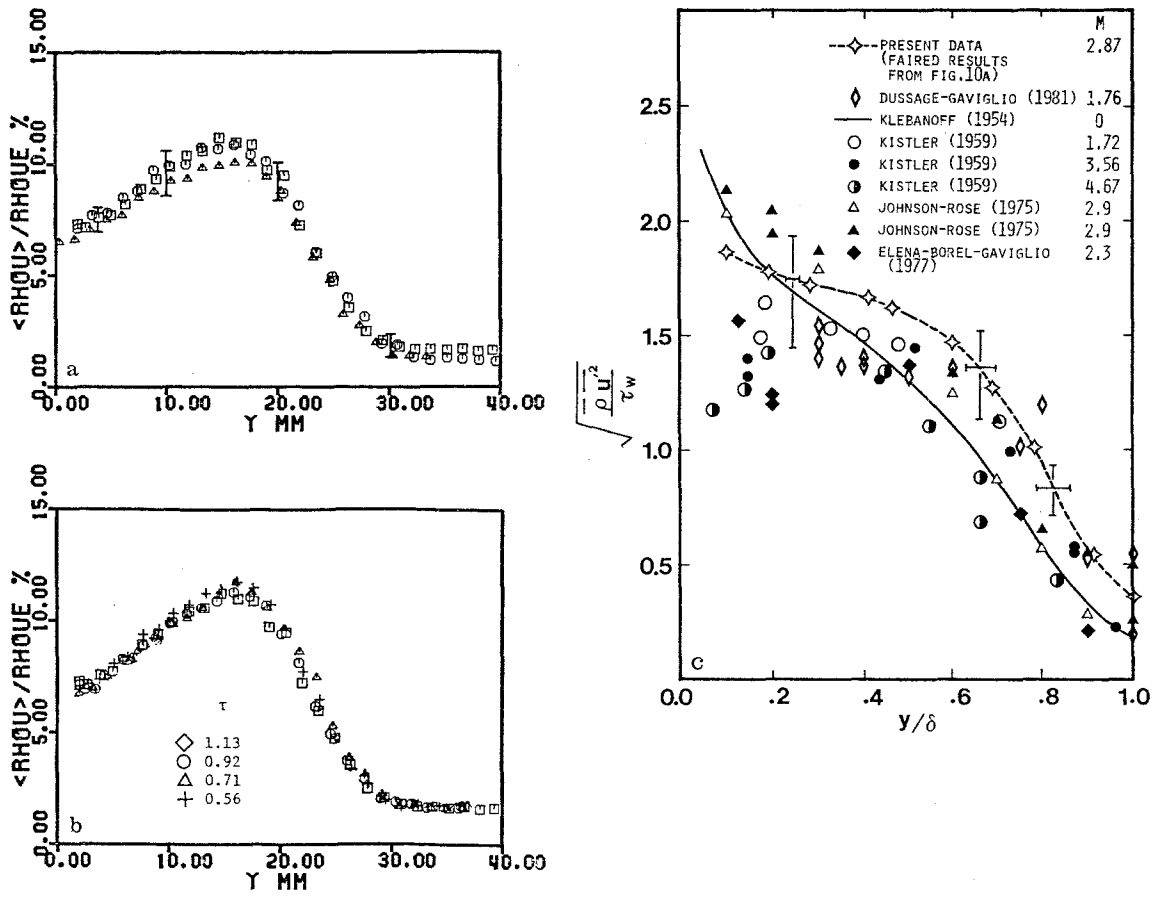

Fig. 10 a–c. **a** rms mass-flow fluctuation intensity for zero pressure gradient $M_a = 2.9$ turbulent boundary layer ($R_\theta = 77{,}600$, $\delta = 26$ mm, $C_f = 0.0011$). Results are for three different wires with overheat ratio ≈ 1.0. **b** rms mass-flow fluctuation intensity for zero pressure gradient $M_a = 2.9$ turbulent boundary layer ($R_\theta = 77{,}600$, $\delta = 26$ mm, $C_f = 0.0011$). Results are for a single wire, with varying overheat ratio. **c** A comparison between the inferred rms velocity fluctuation intensity (deduced from the results given in Fig. 10a) and some representative data reproduced from Dussauge and Gaviglio (1981)

The results are shown in Fig. 10. To deduce the turbulence intensity $\overline{u'^2}$ ($=\langle u' \rangle$) (Fig. 10b), we invoked Morkovin's (1962) "Strong Reynolds Analogy", that is,

$$\frac{\sqrt{\overline{\varrho'^2}}}{\bar{\varrho}} = (\gamma - 1)\, Ma^2 \frac{\sqrt{\overline{u'^2}}}{\bar{U}}$$

This analogy implicitly assumes that the instantaneous total temperature is constant and the pressure fluctuations are negligibly small. Hence, for small fluctuations,

$$\frac{\overline{u'^2}}{\bar{U}^2} = \frac{\overline{(\varrho u)'^2}}{(\overline{\varrho U})^2} \{1 + 2 R_{\varrho u} (\gamma - 1) Ma^2 + [(\gamma - 1) Ma^2]^2\}^{-1}$$

where $$R_{\varrho u} = \frac{\overline{\varrho' u'}}{\sqrt{\overline{\varrho'^2}}\sqrt{\overline{u'^2}}}$$

The correlation coefficient $R_{\varrho u}$ was taken to be constant across the boundary layer and equal to 0.8 (see, for example, the measurements of Dussauge and Gaviglio, 1981).

Before commenting on the data themselves, we need to consider the experimental uncertainties associated with Fig. 10. An error analysis indicates that the measurements were subject to both random and systematic errors. The random errors were associated with uncertainties in evaluating the sensitivity from the calibration curve and correcting the sensitivity for variations in stagnation temperature, in addition to the possibility of a drift in the hot-wire characteristics. Systematic errors included neglecting temperature fluctuations and mean stagnation temperature changes through the flow-field, as well as the errors due to the limited spatial and temporal resolution of the hot-wire system. These errors obviously varied through the flow-field, but an upper bound on the accuracy of $\overline{(\varrho u)'^2}$ may be estimated quite easily. For the present experiment this estimate gave a possible error in $\overline{(\varrho u)'^2} / (\overline{\varrho U})^2$ of -10% to $+19\%$, corresponding to the vertical error bars in Fig. 10a; the horizontal error bars primarily indicate the uncertainty in finding the boundary layer thickness. The results for $\overline{u'^2}$ are subject to errors in the use of the strong Reynolds analogy, and the uncertainty in determining the local Mach number. These considerations, together with the uncertainty in C_f, gave an error

band for $(\bar{\varrho}\, u'^2)/(\varrho_w\, u_\tau^2)$ measurements of -20% to $+36\%$, corresponding to the vertical error bars given in Fig. 10c.

Consider the data presented in Fig. 10. Figure 10a shows the mass-flow turbulence intensity as measured by three different wires, each operated at an overheat ratio of approximately 1.0. The repeatability of the measurements is obviously very satisfactory. The effect of varying the overheat ratio is demonstrated in Fig. 10b. Clearly, the data reach an asymptotic level as the overheat ratio increases, suggesting that the results taken at high overheat are not significantly "contaminated" by total temperature fluctuations.

The inferred velocity fluctuation intensity is shown in Fig. 10c. The present measurements appear to be a little higher than most comparable data, particularly near the wall. The relatively high levels shown by our results may be due to the good spatial and temporal resolution of our measurements; significantly, our measurements agree well with the data of Johnson and Rose (1975) who used both LDV and hot-wire systems.

In conclusion, the overall trend shown by our data, and the level of quantitative agreement with previous data appears to be satisfactory.

5 Conclusions

We have demonstrated that the constant-temperature hot-wire anemometer is inherently unsuitable for measuring turbulent temperature correlations; the major reason is the non-linearity of the temperature sensitivity at low overheat ratios. The instrument is therefore restricted to measurements of the mass-flow fluctuations. If temperature fluctuations are present, high overheat ratios are desirable to avoid contamination of the mass-flow signal by contributions from the fluctuating temperature. Very high overheat ratios may be required if we wish to ignore these contributions entirely.

The maximum frequency response of the system depends on the anemometer roll-off frequency, the spatial resolution of the probe and the maximum A/D conversion rate. The maximum frequency response required depends on the experiment; all requirements on the frequency response become less stringent as the typical size of the shear layer increases.

It was found that the static calibration of the anemometer could be adequately represented by a modified King's Law. This calibration is a function of mean stagnation temperature and corrections are required to account for this dependence if the stagnation temperature varies with time, or with position in the flow field. The corrections were found to be significant, and a satisfactory correction procedure was suggested.

To demonstrate the constant-temperature hot-wire technique in practice, the mass-flow fluctuation levels in a Mach 2.9 turbulent boundary layer were measured. A comparison with comparable data showed satisfactory agreement.

Acknowledgement

This work was supported by NASA Headquarters, Grant No. NAGW-240, monitored by Dr. G. Hicks. The authors would like to thank Dr. D. Bestion of the Institut de Mecanique Statistique de la Turbulence for suggesting improvements to the nonlinear analysis presented in Section 3, and Dr. J-P. Bonnet of the Universite de Poitiers, and Professor P. Freymuth of the University of Colorado for comments on an earlier version.

References

Bonnet, J. P. 1982: Etude theorique et experimentale de la turbulence dans un sillage supersonique. Ph. D. Thesis, L'Université de Poitiers, Poitiers, France

Dussauge, J. P.; Gaviglio, J. 1981: Bulk dilatation effects on Reynolds stresses in the rapid expansion of a turbulent boundary layer at supersonic speed, p. 2.33. Proc. Third Symp. on Turbulent Shear Flows, Univ. of Calif. Davis

Elena, M.; Borel, A.; Gaviglio, J. 1977: Interaction couche-limite turbulente – Onde de choc – Première partie – couche-limite initiale, dispotif d'expérience. O.N.E.R.A. Rep. 15/1455

Freymuth, P. 1977: Electronic testing of frequency response for thermal anemometers. TSI Quarterly 3, 5–12

Freymuth, P. 1981: The effect of varying resistance ratio on the behavior of constant-temperature hot-wire anemometers. J. Phys. E: Sci. Instr. 14, 1373

Johnson, D. A.; Rose, W. C. 1975: Laser velocimeter and hot-wire anemometer comparison in a supersonic boundary-layer. AIAA Journal 13, 512–515

Kistler, A. 1959: Fluctuation measurements in a supersonic turbulent boundary layer. Phys. Fluid 2, 290–296

Klebanoff, P. S. 1954: Characteristics of turbulence in a boundary layer with zero pressure gradient. NACA TN3178

Kovasznay, L. S. G. 1950: The hot-wire anemometer in supersonic flow. J. Aero Sciences 17, 565–573

Laufer, J.; McLellan, R. 1956: Measurement of heat transfer from fine wires in supersonic flow. J. Fluid Mech. 1, 276

Morkovin, M. V. 1956: Fluctuations and hot-wire anemometry in compressible flows. AGARDograph 24

Morkovin, M. V. 1962: Mecanique de la turbulence. Favre, A., Ed., C.N.R.S., Paris, pp. 367–380

Perry, A. E.; Morrison, G. L. 1971: A study of the constant-temperature hot-wire anemometer. J. Fluid Mech. 47, 577–599.

Perry, A. E.; Smits, A. J.; Chong, M. S. 1979: The effects of certain low frequency phenomena on the calibration of hot-wires. J. Fluid Mech. 90, 415–431

Settles, G. S.; Fitzpatrick, T. J.; Bogdonoff, S. M. 1979: Detailed study of attached and separated compression corner flowfields in high Reynolds number supersonic flow. AIAA J. 17, 579–585

Smits, A. J. 1974: Further developments of hot-wire and laser methods in fluid mechanics. Ph. D. Thesis, University of Melbourne, Melbourne, Australia

Smits, A. J.; Muck, K. C. 1983: Constant temperature hot-wire anemometer practice in supersonic flows, Part 2: The inclined wire. AIAA Paper 83-0508. Exp. Fluids (submitted)

Smits, A. J.; Perry, A. E. 1980: The effect of varying resistance ratio on the behaviour of constant temperature hot-wire anemometers. J. Phys. E: Sci. Instr. 13, 451–456

Smits, A. J.; Perry, A. E.; Hoffmann, P. H. 1978: The response to temperature fluctuations of a constant-current hot-wire anemometer. J. Phys. E: Sci. Instr. 11, 909–914

Wyngaard, J. C. 1968: Measurements of small-scale turbulence structure with hot-wires. J. Phys. E: Sci. Instr. 1, 1105

Received February, 11, 1983